THE INFLUENCE OF FLIGHT SPEED, IMAGE OVERLAP, AND LIGHTING CONDITIONS ON THE SPATIAL ACCURACY AND DEVELOPMENT TIME OF LOW-COST UAS IMAGING

Madeline Hower
Virginia Tech, Blacksburg, VA, 24060, USA

Widespread emerging UAV technology has resulted in an increased use of drones across a variety of fields to complete mapping and surveying evaluations. However, accessible guidelines providing information on the effects parameter choices and environmental considerations have on orthomosaic quality and accuracy do not exist. To improve the understanding of the various influences on mapping results, this study evaluates how image overlap ratio, mapping speed, and lighting conditions affect spatial accuracy and development time for resulting orthomosaic images. This evaluation was done by conducting mapping missions with several parameter variations over a homogeneous area and a non-homogeneous area. The accuracy was assessed by calculating the root mean square error (RMSE). The results suggest that effects of mapping parameters differ between homogeneous and non-homogeneous areas. For a homogeneous location, the most accurate conditions were obtained by conducting mapping on a clear weather day, with a 60/80 overlap, at a mapping speed of 3 m/s. For the non-homogeneous location, the most accurate conditions were conducting mapping on a cloudy weather day, with a 70/80 overlap, at a mapping speed of 5m/s. A correlation was also found between lighting conditions and image development time and between image overlap and image development time, where clear day weather resulted in a lower processing time and reducing front overlap had the greatest reduction in processing time.

Abbreviations

UAV	=	Unmanned Aerial Vehicle
UAS	=	Unmanned Aircraft System
AGL	=	Above Ground Level
GCPs	=	Ground Control Points
NIR	=	Near-Infrared
NDVI	=	Normalized Difference Vegetation Index
GSD	=	Ground Sample Distance
RC	=	Remote Controller
RMSE	=	Root Mean Square Error

I. Introduction

Unmanned aircraft were first designed for use in military applications. Since their creation, their uses have expanded to encompass widespread civilian applications, from providing entertainment[1] to assisting in rescue missions[2]. A UAS is now a commonplace tool in data acquisition for a variety of fields. Instead of traditional photogrammetric methods, researchers are now turning to UAS to produce imagery data more efficiently. The use of drones to capture images also allows the user to view a large area with significant accuracy. Combining the mapping capabilities of UAS with multispectral imaging aids users in monitoring crops and vegetation, military target tracking and land mine detection, environmental monitoring, and surveying.

Multispectral imaging captures images at several different wavelengths on the electromagnetic spectrum. Typically, four different bands are captured: blue (450 - 490nm), green (540 - 580nm), red (630 - 680nm) and NIR (750 - 950nm).

Utilizing these bands, the NDVI can be calculated via Eq. (1).

$$NDVI = (NIR - red) / (NIR + red) \quad (1)$$

NDVI can be used to monitor crops and vegetation health as well as identify areas of drought[3].

Utilizing a post-processing software, images captured from a drone can be stitched together to form an orthomosaic. An orthomosaic is a georeferenced image mosaicked from a collection of images. This results in an undistorted image of an area that shows accurate dimensions. Orthomosaics can be used for a variety of purposes where geospatial analysis or precise measurements are necessary. An orthomosaic provides a more accurate representation of an area than a photo of that area may provide.

Accurate surveying and mapping is a vital component of ensuring your data is reliable and precise. The overall accuracy of an orthomosaic image is dependent on three major components:

(1) Post-processing software
(2) Drone mapping parameters
(3) Environmental Considerations

When imaging with drone technology, several parameters chosen before and during mapping can greatly impact the accuracy of the resulting data including the camera and sensor quality, use of GCPs, flight speed, overlap of images, and drone altitude. While research has shown that these parameters do affect the overall quality of the resulting orthomosaics[5], information is lacking regarding the effect a change in one of these parameters has on the overall accuracy of the data. The accuracy needed for the collected data depends on the use application. In many applications, it is not necessary for the result to have maximum accuracy. In this case, using the optimal parameters will result in unnecessary additional time and effort during the mapping and post-processing stages.

Minimizing the amount of time spent collecting and generating final images is important to consider when mapping. Changes in parameters may greatly decrease the flight and image processing time, which can result in a significant reduction in cost. A shorter survey time also increases the accuracy of the final product as there is less time for fluctuations in lighting, wind speed, and other environmental factors during mapping. In larger survey areas that take greater amounts of time to map properly, it may be necessary to adjust parameters to reduce the survey time to accommodate a UAVs battery life.

This study aims to provide a guide for those wishing to complete multispectral mapping on the effect a change in lighting condition, flight speed, or image overlap may have on overall spatial accuracy and development time*, to better inform mapping decisions and techniques.

*For the purposes of this study, development time is used to refer to the combined surveying and image processing time of each test.

II. Test Methodology

This section discusses the process used to create orthomosaic images for each test and the analysis used to determine their accuracies. The methodology is divided into four phases: data preparation, data collection, data processing, and error analysis and is based off a methodology proposed by Ref. 6. An overview of this process is shown in Figure 1.

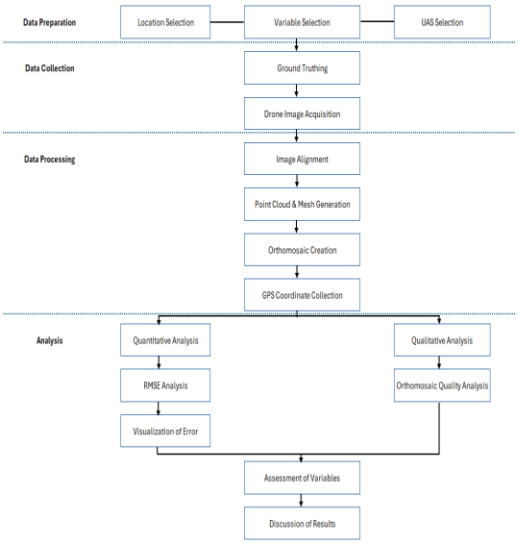

Figure 1: Study Methodology

A. Data Preparation

1. Location Selection

Two different testing areas were selected for this study. Both areas are located at the Heritage Community Park in Blacksburg, VA.

The first location, which will represent a homogeneous area, had a testing area of 6,400 square meters. The area was chosen for its consistent landscape and can be described as an undeveloped field with minimal altitude change, Figure 2.

Figure 2: Homogeneous Location Test Area

The second test location, representing a non-homogeneous area, has a testing area of 5,100 square meters. This area was chosen for its series of features including open areas, trees, shrubbery, and buildings, Figure 3. Like the first testing area, this location is undeveloped with minimal altitude change.

Figure 3: Non-Homogeneous Location Test Area

2. Variable Selection

Parameters used during image collection can greatly affect the quality of a resulting orthomosaic. These parameters include flight altitude, number of GCPs used, image overlap ratios, flight speed, and light intensity.

Constant Parameters:

Flight Altitude: Flight altitude is the height from the ground that imagery is taken from the drone. The DJI Mavic 3M has terrain-following capabilities that control the drone's altitude while mapping. According to studies on flight altitude for mapping accuracy, error has been found to increase with an increase in flight altitude[7]. It is important to ensure that a chosen flight altitude will result in good spatial resolution, which corresponds to a low ground sample distance. GSD can be found using Eq. (2),

$$GSD = \frac{Flight\ Height * Sensor\ Width}{Focal\ Length * Image\ Width} \quad (2)$$

The flight altitude was set to 100 ft AGL and kept consistent for all tests in this study. This led to a resulting GSD of 1.41cm/pixel. This is well under the 10cm/pixel maximum GSD specified by Ref. 8 for adequate spatial resolution in UAV surveying.

Number of GCPs: Ground control points (GCPs) are points on the ground of the surveying area that have a known geographic location. They are used to define area boundaries and scale the area between points. It has been shown that having the right number of

GCPs in the correct locations can greatly improve accuracy[9]. The results of Ref. 10 show that there are no significant accuracy improvements after increasing the number of GCPs past 3[10]. The references also show the best positioning for the GCPs are on the external borders and the center of the mapping site[11]. For this study, five GCPs were used, with four surrounding the boundaries of the survey area and one placed near the center of the survey site.

Varied Parameters:

Image Overlap Ratios: Refs. 8, 12, and 13 have studied the influence of image overlap on image quality. The overlap ratio is an important parameter to consider for mapping and surveying because a high overlap ratio can correspond to lengthy process times while a low overlap ratio can result in gaps in the final image[13]. DJI suggests a default overlap ratio of 70/80 (Side/Front)[14]. The overlap ratios used in this study include side-to-front ratios of 70/80, 60/80 and 70/70 to create comparisons of resulting images with 10% difference in front or side overlap.

Flight Speed: During a mapping mission, flight speed is an integral parameter to consider. A flight speed that is too fast may lead to lower quality results as there may not be enough data, while a slower flight speed may lack efficiency. The proper flight speed range for mapping varies based on the UAV used. The DJI Mavic 3M had a possible mapping range between 1 and 6 m/s. Two flight speeds were used in this study: 3 and 5m/s.

Light Intensity: According to Ref. 15, poor lighting conditions can significantly decrease the quality and therefore the accuracy of UAS generated images[15]. The lighting conditions for this study are grouped into three categories: clear, cloudy, and overcast. Table 1 shows each of these lighting categories and their corresponding range of light intensity.

Table 1: Lighting Condition Ranges

Lighting Condition	Light Intensity Range [Klux]
Overcast	0.8 – 3.0
Cloudy	30 – 60
Clear	60 - 100

Table 2 provides an overview of the different mapping parameters used during this study.

Table 2: Mapping Variables

Parameter	Value
Flight Altitude [ft AGL]	100
Number of GCPs	5
Flight Speed [m/s]	3
	5
Image Overlap (Side/Front)	70/80
	70/70
	60/80
Lighting Condition	Overcast
	Cloudy
	Clear
Test Area Location	Field – Homogeneous
	Shrub – Non-Homogeneous
Wind Speed [mph]	3 – 5
Time of Day	11:00 – 13:00

The prescribed constant conditions are assumed constant throughout the testing period. However, several of these conditions will vary during and between mappings. Solar intensity will change with solar movement and cloud movement. To mitigate these variations, all testing was completed between 11:00 – 13:00 where the sun is directly overhead and there is minimal change in shadow direction. Smaller mapping areas were chosen to shorten the mapping time and minimize cloud movement variations during surveys.

Wind speed also fluctuated during mapping missions. This was monitored throughout each survey to ensure the variation was minimal. Mapping was only conducted in low wind speeds between 3-5mph.

3. UAS Selection

Imagery for this study was collected with a DJI Mavic 3 Multispectral, a low-cost UAV designed primarily for agricultural and environmental surveying applications, Figure 4. The Mavic 3M weighs 951g and is equipped with a GNSS receiver, a built-in RGB camera and four multispectral cameras: red, green, red edge, and near-infrared[16]. The RGB camera has a 20MP resolution and 5280×3956 pixels. The multispectral cameras have a 5MP resolution and 2592×1944 pixels.

Figure 4: DJI Mavic 3 Multispectral and DJI Remote Controller Pro

A paired RC controls the UAV. Flight planning was conducted on the RC using DJI Pilot 2. The image format from the RGB camera was stored as RAW .JPEG files, and the multispectral images were stored as .TIF files.

B. Data Collection

1. Ground Truthing

Ground truthing is the collection of information by direct observation and measurement which is known to be true.

Prior to each mapping mission set, 5 GCPs were placed in the testing area, and their exact locations were documented. These GCP locations were measured using a GNSS Land Meter. This device uses GNSS with GPS, BDS, GLONASS, GALILEO, and SBAS and has an accuracy of .1m. To improve random error, 5 separate measurements were taken at each GCP location and averaged. These ground measurements were compared to the data collected from the drone imagery to determine orthomosaic error.

2. Drone Image Acquisition

During each flight test, the weather conditions (wind speed, visibility, and temperature), total flight time, number of images taken, flight speed, image overlap, and solar radiance were recorded. The drone used GNSS with GPS, Galileo, and Bei Dou, with at least 22 connected satellites during each flight. A total of 18 tests were performed at each testing site.

Mapping was completed using the DJI Pilot 2 app on the Mavic 3M controller. Figure 5 shows the drone flight area, mapping route, and GCP placement locations for the homogeneous area.

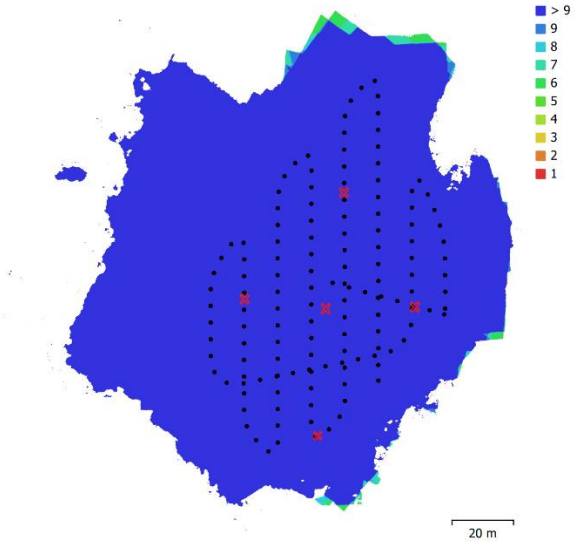

Figure 5: UAV Mapping Route- GCP Locations are indicated with red X's and the blue color indicates an image overlap greater than 9 images

C. Data Processing

The images gathered during data collection were post-processed in Agisoft Metashape. For each test conducted, images were added and aligned, the camera locations were optimized and fitted, a dense point cloud was created, mesh was generated, and orthomosaic formed. After its creation, the orthomosaic was imported into QGIS as a layer and GPS coordinates were gathered for each GCP on the orthomosaic.

Image Alignment: In the image alignment step, an algorithm is used to detect tie points in the 2D images captured by the drone and match them together. A tie point limit is the upper limit of matching points for every image. A tie point limit too low may result in parts of the dense point cloud model to be missing. Agisoft recommends this value to be 4,000. The tie point limit for the processing of the data in this study was set to 10,000.

After image alignment, the cameras are optimized. Several parameters were optimized including the x- and y- dimension focal lengths (pixels), coordinates of lens optical axis interception with sensor plane, the skew transformation coefficient, radial distortion coefficients, and tangential distortion coefficients.

Additional information on the algorithms used to perform alignments and optimizations is provided by Refs 17 and 18.

After the images are aligned, the coordinates for the GCPs placed in the testing area were imported into Agisoft as reference points.

Point Cloud & Mesh Generation: A dense point cloud is built computing depth information for each camera and combining these into the same datum. The resulting single dense point cloud is then used as an input for mesh generation.

From this input, a mesh is generated that fills in the gaps within the dense point cloud and provides a more comprehensive visualization of the model. Agisoft will then use this mesh to build the orthomosaic.

Orthomosaic Creation: The orthophotos are stitched together into one final orthomosaic, using the previously made mesh as an input.

GCP Coordinate Collection: After the orthomosaic was generated, it was exported as a .TIF file. These images were imported into QGIS as layers, and the coordinates for each of the GCP locations were obtained and documented.

D. Analysis

Accuracy evaluation across the orthomosaic photos was based on the variation between the UAV obtained coordinate values and the measured values obtained during ground truthing. The RMSE is frequently used as a quantitative measure of accuracy due to its interpretability and sensitivity to outliers. This analysis methodology is based off the methodology used by Refs 4-8, 10, 11, and 13.

The root mean square error is the quadratic mean of the differences between the observed values and predicted ones, given in Eqs. (3), (4), and (5) where (x_{ortho},y_{ortho}) are the x and y GCP coordinates obtained from the orthomosaics and (x_{GT},y_{GT}) are the x and y coordinates obtained from ground truthing. This is a measure of accuracy, where a 0 value would indicate a perfect fit to the data. Since this value is non-negative, a lower value indicates better accuracy.

$$RMSE = \sqrt{M_X^2 + M_Y^2} \quad (3)$$

$$M_X = \sqrt{\frac{\sum_{i=1}^{n}(X_{ORTHO} - X_{GT})^2}{n}} \quad (4)$$

$$M_Y = \sqrt{\frac{\sum_{i=1}^{n}(Y_{ORTHO} - Y_{GT})^2}{n}} \quad (5)$$

A qualitative analysis of orthomosaic quality was also conducted to note any visual effects of the tested parameters on resulting quality.

III. Results and Discussion

36 mapping missions were completed in two separate locations with variations in lighting conditions, speed, and image overlap. Each variation resulted in changes in the overall error for the resulting orthomosaic. Table 3 shows the RMSE for each test under the varying parameters.

Table 3: RMSE [m] for each test set

	Homogeneous Location		Non-Homogeneous Location	
Overcast	**3 m/s**	**5 m/s**	**3 m/s**	**5 m/s**
70/80	1.1318	1.2171	3.0515	3.4380
60/80	1.1095	1.2531	3.3352	3.5965
70/70	1.2659	1.4211	3.5056	3.3640
Cloudy				
70/80	1.7873	1.7597	0.9456	0.8827
60/80	1.4683	1.564	0.8766	1.2982
70/70	1.5079	1.506	1.1422	1.1364
Clear				
70/80	0.8440	0.9663	3.7414	3.3570
60/80	0.7969	0.7907	3.4352	3.7164
70/70	1.0848	1.4740	3.8333	3.7218

RMSE ranged between 0.79m and 3.83m, where the lowest error was obtained on a clear day with a 60/80 overlap and a 5m/s mapping speed in the homogeneous surveying area and the highest error occurred in the non-homogeneous area on a clear day, with a 70/70 overlap and at 3m/s.

A. Location Analysis:

Qualitative Discussion: The orthomosaics created of the homogeneous testing area were all complete with no gaps in the targeted mapping area, Figure 6.

Figure 6: Homogeneous Area Orthomosaic

All images produced were clear and each of the GCP coordinates were visible. This verifies that all parameter combinations utilized during tests were appropriate settings for the orthorectification process of the homogeneous location.

The orthomosaics created for the non-homogeneous location testing area contained several gaps in the final image. These gaps were found to be at the locations of dense vegetation within the mapping area. Several attempts were made to improve these results through changes in post processing settings, including gap filling, and increasing tie points. These changes did not result in improved orthomosaic results. It is likely that the mapping parameters used on this location did not provide enough data for the areas of more dense coverage to be accurately represented. Tests with lower overlap resulted in a greater number and larger gaps in the orthomosaic, Figure 7.

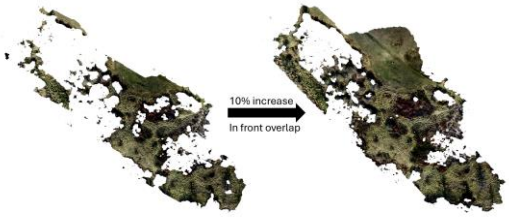

Figure 7: Overlap Effects on Orthomosaic Quality

To acquire a complete set of images for this non-homogeneous location, image overlap would need to be increased. This would provide more overlap between each image, yielding more data to create the model more completely.

Five of the orthomosaics produced for the non-homogeneous tests had holes in the locations of their GCP's. These tests were not used in analysis.

The significant quality difference between the homogeneous and non-homogeneous orthomosaics under the same mapping parameter choices indicates that mapping parameters affect orthomosaic creation differently for different landscapes, and coverage of the surveying area must be appropriately considered when making parameter choices.

Quantitative Discussion: Plots of the average RMSE values for each configuration of image overlap (Figure 8a), mapping speed (Figure 8b), and lighting conditions (Figure 8c) during mapping in each test location shows that there is a significant difference in error between the two locations. The non-homogeneous location had a higher error value than the homogeneous location for all but one testing condition.

Differences in RMSE between tests in the homogeneous and non-homogeneous areas with the same parameter settings ranged from 0.92m to

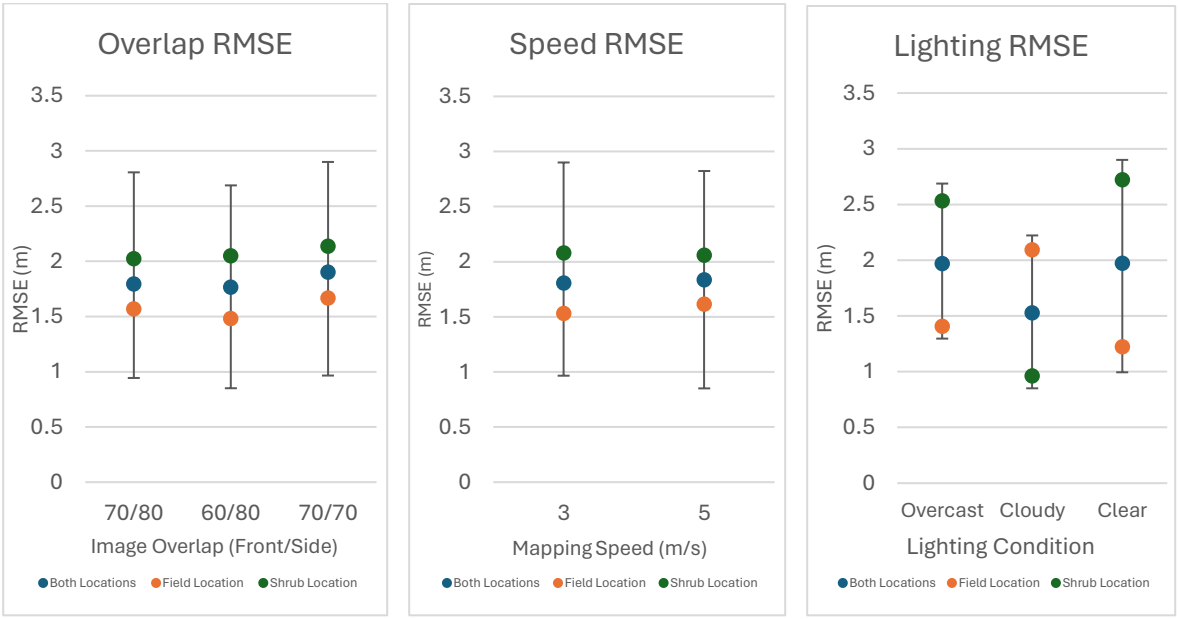

Figure 8: Average RMSE's with respect to each overlap condition (a), speed condition (b), and lighting condition (c) across homogeneous test sets, non-homogeneous test sets, and all test sets.

1.73m. The differences in homogeneous and non-homogeneous accuracies were similar regardless of image overlap or mapping speed used. However, lighting condition impacted the difference in error between the homogeneous and non-homogeneous locations. An overcast day resulted in accuracy differences between the two locations from 0.92 – 1.27m. A cloudy day resulted in a higher accuracy difference, ranging from 1.04 – 1.67m. The highest differences found between non-homogeneous and homogeneous landscapes were during clear day conditions, where the difference ranged from 1.21 – 1.73m.

This indicates that if collecting drone imagery across several locations, an overcast day would be the best lighting condition for consistent accuracy across areas. An overcast day does not cast shadows that decrease the accuracy of the orthomosaic during post processing. Clear skies can create harsh shadows, which would impact the non-homogeneous area much more than the homogeneous area as it contains vegetation and structures that could cast shadows during mapping.

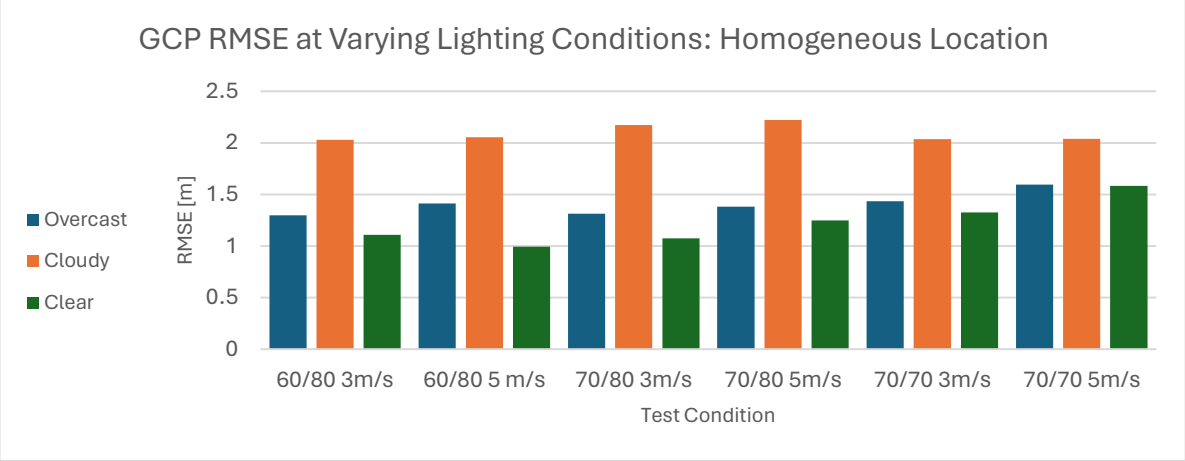

Figure 9: RMSE across GCP's in each test for varying lighting conditions in the homogeneous area.

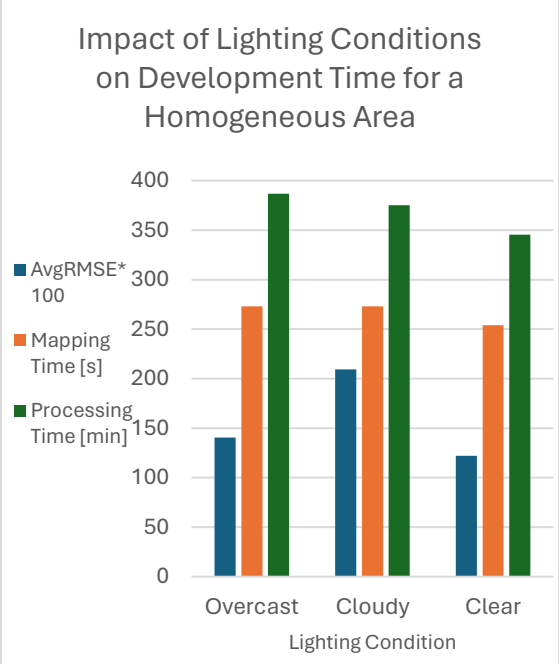

Figure 10: Average image processing and mapping times for the homogeneous area lighting conditions.

B. Lighting Condition Analysis

It can be shown that for all tests in the homogeneous location, cloudy conditions yielded the results with the most error, with an average error of 2.09m. Testing in clear conditions resulted in the lowest error, which was an average error of 1.22m, a difference of 0.87m from the cloudy day error. This may be due to clear weather providing a more consistent lighting intensity throughout testing. In a field, with nothing to cast a shadow in the mapping area, the uniform lighting throughout the mapping period will offer a more accurate mapping.

The cloudy day weather resulted in more fluctuation in lighting during each mapping than the clear day weather, which impacted the overall orthomosaic image quality, Figure 9. This fluctuation was caused by the movement of clouds while the mapping mission took place. The difference in error from one

GCP to another is seen to be much larger on a cloudy day because of this cloud movement.

For the homogeneous area, lighting condition changes had no significant effect on mapping time. This is expected as the drone will follow the same settings regardless of the weather conditions. Differing lighting conditions did influence the image processing time of the orthomosaic rendering, Figure 10. The clear weather condition tests had a shorter image processing time (345min) than the overcast (386min) and cloudy (375min) conditions.

minutes and decreased average error by 1.57m, Figure 12.

The results obtained indicate that the ideal lighting condition for conducting mapping missions of homogeneous regions is a clear weather day, and the ideal lighting condition for non-homogeneous region mapping is a cloudy day. Choosing test days based on this suggestion would likely result in a reduction in both error and development time.

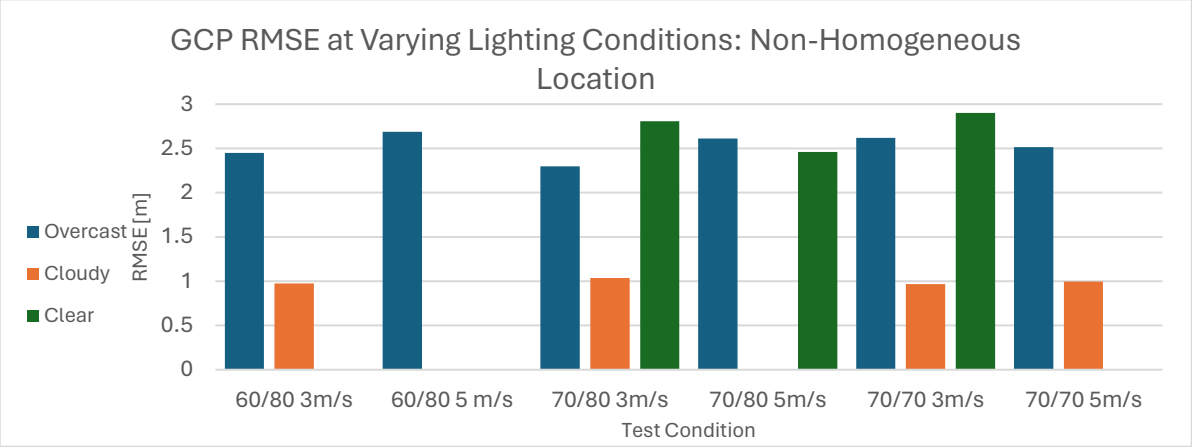

Figure 11: RMSE across GCP's in each test for varying lighting conditions in the non-homogeneous area.

Choosing a clear day to perform homogeneous area mapping over an overcast day minimized average overall development time by approximately 41 minutes and average error was reduced by approximately 0.18m.

The trend between lighting condition and RMSE in the non-homogeneous area differed from the homogeneous trends. The cloudy day tests resulted in a smaller error (0.97m) than that of the clear day tests (2.9m), Figure 11. On a clear day, objects cast noticeable shadows on the ground, and an area dense with trees and shrubbery will contain many shadows that will decrease the accuracy of the mapping.

The non-homogeneous area showed the same correlations between lighting conditions and development times as the homogeneous area, where there is no relationship between lighting conditions and mapping time and where clear skies results in a shorter image processing time.

Choosing a cloudy day to perform mapping in a non-homogeneous area rather than an overcast day decreased overall average development time by 11

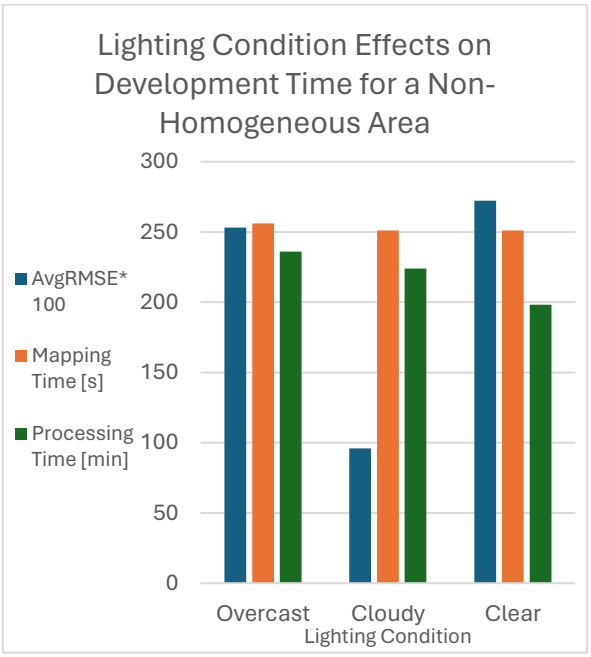

Figure 12: Average image processing and mapping times for the non-homogeneous area lighting conditions.

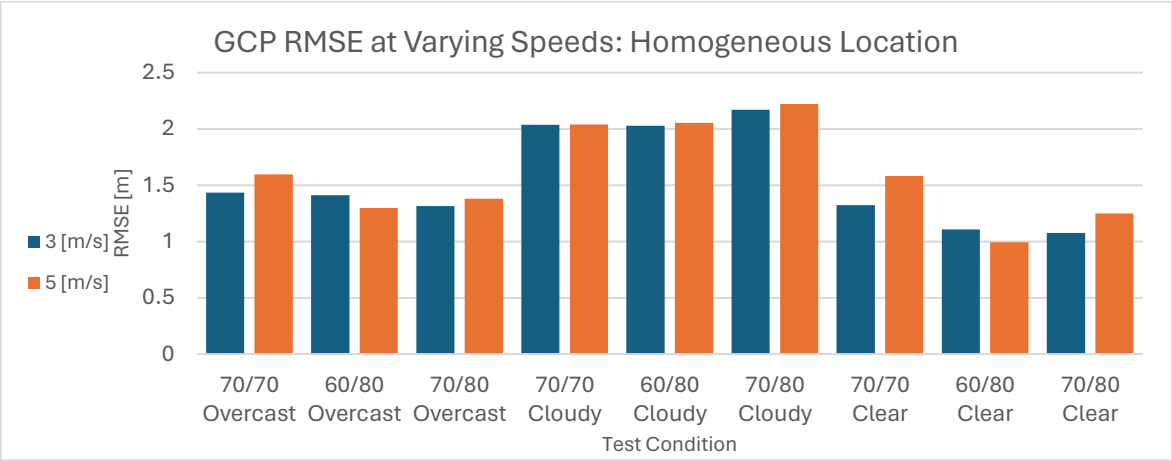

Figure 13: RMSE across GCP's in each test for varying mapping speeds in the homogeneous area.

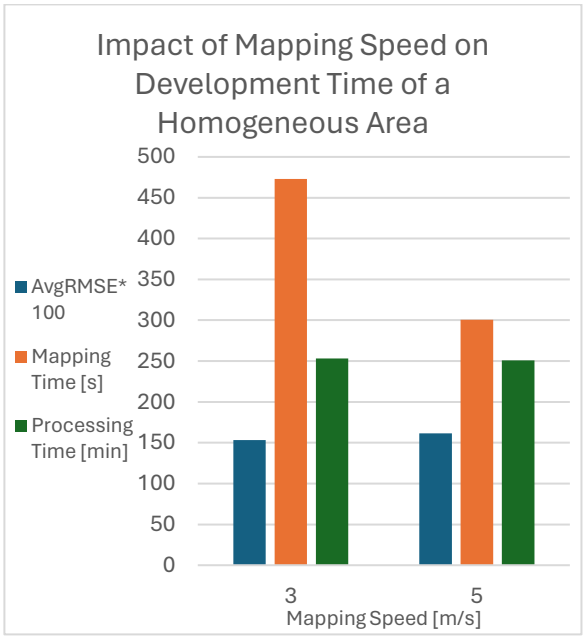

Figure 14: Average image processing and mapping times in the homogeneous area for varying mapping speeds.

C. Mapping Speed Analysis

An increase in mapping speed when mapping a homogeneous area resulted in an error increase for 8 of the 9 tests, Figure 13. The test cases that decreased in error did so by less than 0.02m. The average error increase with a 2m/s mapping speed increase for all tests was 0.08m, with the greatest increase in error being 0.26m, which was the test set with a 70/70 overlap on a clear day.

These results suggest that when conducting mapping missions on a homogeneous area, increasing the mapping speed will most likely result in a small increase in error.

The increase of mapping speed resulted in a decrease in the average image processing time of 2 minutes, a decrease in the average mapping time by 2.8 minutes, and a small increase in average error of 0.01m, Figure 14. This result is expected as an increase in speed did not affect the number of images taken during mapping and therefore should not affect the image processing time. The small variation in image processing time is likely due to varying connections to the network storage during each test's processing stages. The images were stored on an external hard drive and accessed during post processing.

The average error increase for non-homogeneous area tests increasing from a 3 to 5m/s mapping speed was 0.02m, Figure 15. Three of the five test sets showed an increase in error while two test sets showed a small decrease. Since the effects of mapping speed increase were so varied, no correlation was able to be determined between the mapping speed and spatial accuracy in the non-homogeneous area.

Non-homogeneous area mapping time decreased by 3 minutes with an increase in mapping speed of 2 m/s and image processing time decreased by 18 minutes, Figure 16.

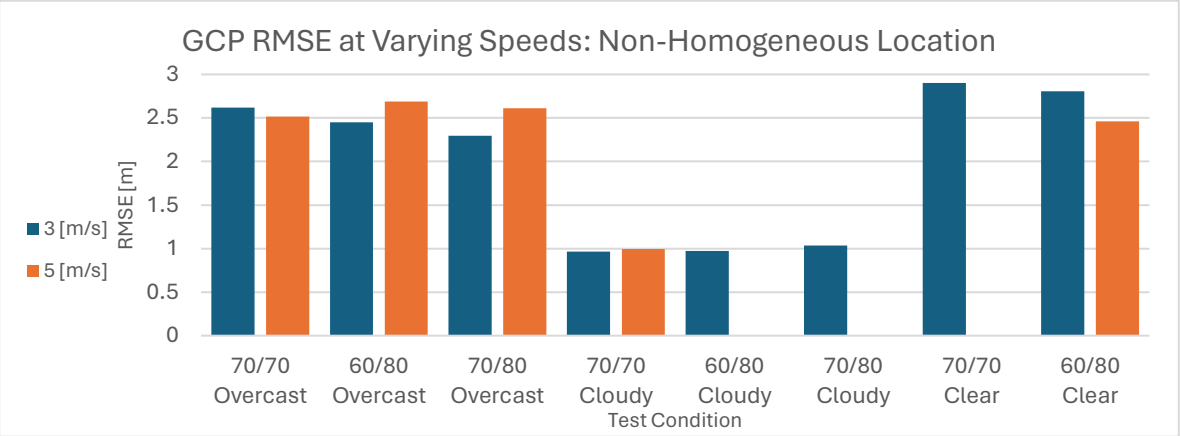

Figure 15: RMSE across GCP's in each test for varying mapping speeds in the non-homogeneous area.

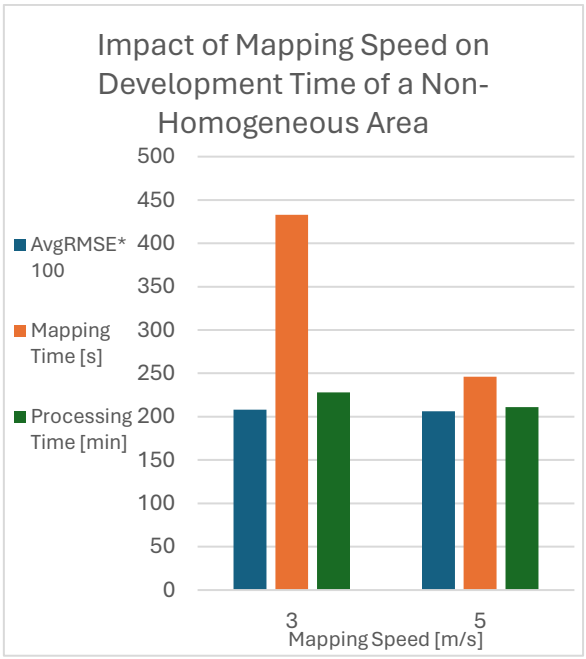

Figure 16: Average processing and mapping times in the non-homogeneous area for varying mapping speeds.

From the comparisons made of mapping speed error and development times, it is suggested that a small increase in mapping speed will not result in any significant difference in error, regardless of the homogeneity of the area being mapped. However, an increase in mapping speed decreases the overall development time of the imagery. The mapping time of the 5m/s tests were much smaller when compared with the 3m/s, but when compared to the decrease in image processing time, is less effective. For the non-homogeneous tests, mapping time was decreased by 43% while image processing time decreased by 8%. However, the 8% decrease saved 18 minutes while the 43% difference only saved 3 minutes. This indicates that for a smaller surveying area, it is more time effective to focus on the reduction of image processing time rather than mapping time.

It is important to point out that the results found for mapping speed in this study depend on the camera photo capture interval. Use of a different UAS for

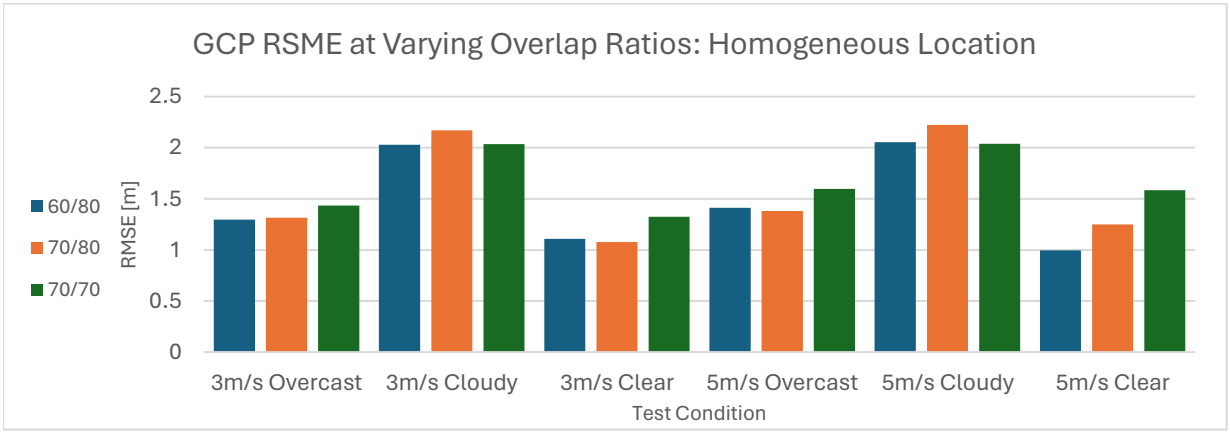

Figure 17: RMSE across GCP's in each test for varying image overlap ratios in the homogeneous area.

mapping will yield different results. This study tests two mapping speeds within the ranges available to the Mavic 3 Multispectral. Careful consideration of shutter speed and corresponding mapping speed ranges is needed to apply this to other systems.

A. Image Overlap Analysis

For a homogeneous location, a side overlap increase of 10% had varying results. Half of the tests saw an increase in error while the other half saw a decrease in error, Figure 17. The average change in error was found to be an increase of 0.08m. These results are not consistent with previous studies that indicate an increase in side-overlap will result in a decrease in error.

A frontal overlap increase of 10% resulted in a decrease of average error by 0.1m. 2 of the 6 test sets saw an increase in error with the 10% increase in frontal overlap.

When side overlap was decreased by 10%, the average image processing time was reduced by 85 minutes and the average mapping time was reduced by 24% (1.6 minutes). This reduction in mapping time is due to the drone following a wider path when crossing along the surveying area.

A 10% decrease of front overlap resulted in a decrease of average image processing time by 167 minutes and a negligible variation in mapping time (Figure 18). No variation in mapping time is expected as the drone will take images at the same speed and with the same pattern as the original overlap condition.

All tests with a decrease in either front or side overlap resulted in an overall decrease in development time. However, decreasing frontal overlap resulted in a higher reduction of development time as significantly fewer images were taken.

For the non-homogeneous location, an increase of side overlap by 10% resulted in an average error decrease of 0.03m while an increase of front overlap by 10% resulted in an average error decrease of

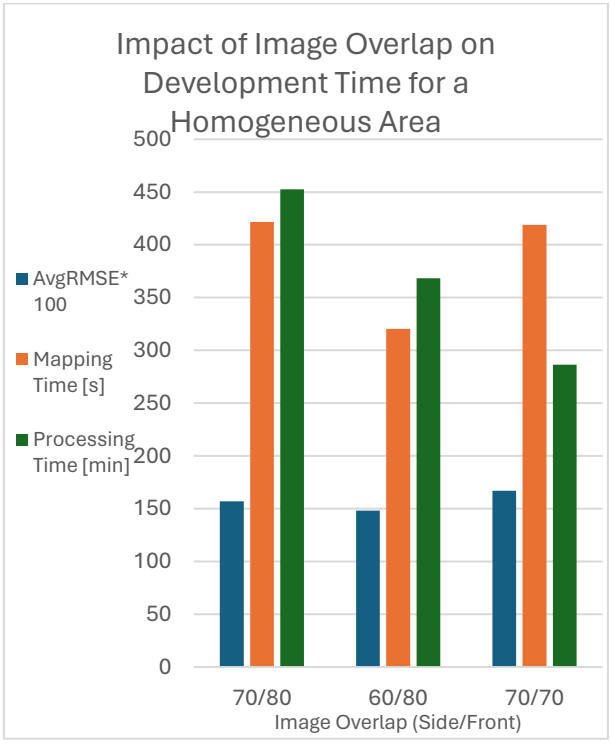

Figure 18: Average image processing and mapping times in the homogeneous area for varying image overlap ratios.

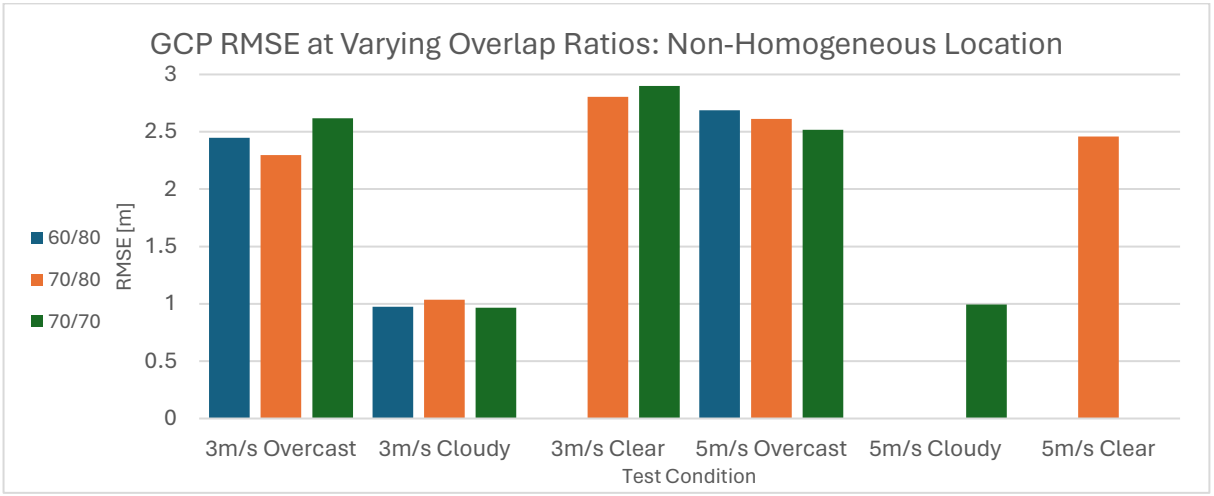

Figure 19: RMSE (boxes) and error range (bars) across GCP's in each test for varying image overlap ratios in the non-homogeneous area.

0.11m, Figure 19. This result is consistent with previous studies that show increasing overlap positively affects orthomosaic accuracy[5]. The higher overlap provides more data for post processing, which allows for better accuracy in the model.

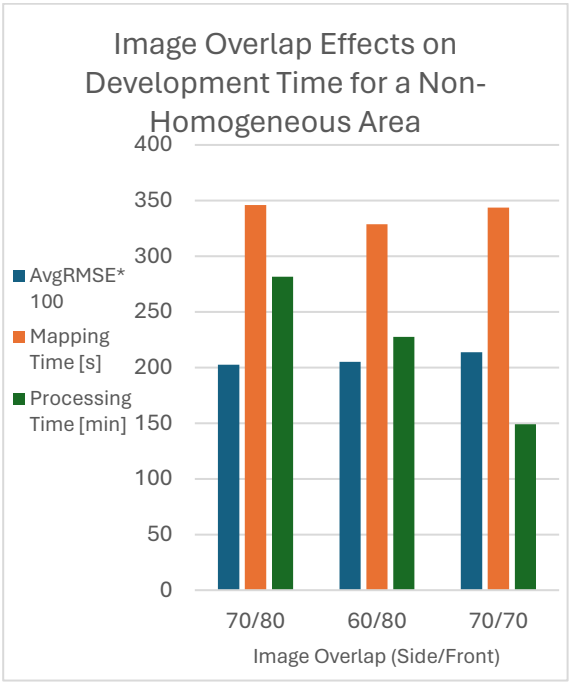

Figure 20: Average image processing and mapping times in the homogeneous area for varying image overlap ratios.

Similarly to the homogeneous location, the non-homogeneous location results showed a decrease in development time with a decrease in overlap ratios, Figure 20. When side overlap was decreased by 10%, image processing time decreased by 2 minutes and mapping time decreased by 30 seconds. When front overlap was decreased by 10%, image processing time decreased by 54 minutes and there was no effect on mapping time.

IV. Conclusion

In this study, various mapping components were evaluated in two locations: an open field area and an area covered with vegetation, to determine how mapping speed, image overlap ratio, and lighting conditions affect the spatial accuracy and development time of resulting orthomosaics. Tests were conducted with a DJI Mavic 3 Multispectral flown at a height of 100ft AGL. 5 GCP's were placed prior to UAV imaging and used to assess spatial accuracy after post-processing. 36 tests were conducted with varying mapping speeds of 3 and 5 m/s, image overlap ratios of 60/80, 70/70, and 70/80, and overcast, cloudy, and clear lighting conditions. It was shown that resulting orthomosaics for the non-homogeneous location had more error than the homogeneous location. The non-homogeneous area also had larger errors for clear weather conditions while the homogeneous location had lower errors for clear weather conditions. Clear weather conditions resulted in shorter development times for all area types.

Mapping speed showed minimal impact to accuracy, and there was no impact of varying speed on overall image processing times.

Decreasing front overlap resulted in a significant decrease in image processing time, with a small increase in overall error.

The results of this study are limited to the use of the DJI Mavic 3 Multispectral for mapping. Use of another UAS will change the results of the study, especially for the effects of changing mapping speed, where shutter speed significantly influences the proper speed values. These trends may not be applicable outside the ranges tested in this study.

The consistently increasing usage of UAV technology for mapping requires further investigations into mapping parameter effects on UAS imagery quality and accuracy. The results of this study aim to assist in the development of more comprehensive guidelines for proper mapping settings in various surveying scenarios.

Acknowledgements

This study is supported by the Virginia Tech Drone Park.

References

[1]La Bella, L., *Inside the World of Drones: Drones and Entertainment*, 1st ed., The Rosen Publishing Group, New York, 2017.

[2]Potka, M., Ptak, S., Kuziora, L., "The Use of UAV's for Search and Rescue Operations," *Procedia Engineering*, Vol. 192, Pg. 748-752, 2017, URL: https://doi.org/10.1016/j.proeng.2017.06.129

[3]"Measuring Vegetation," *NASA Earth Observatory*, 2000, URL: https://earthobservatory.nasa.gov/features/MeasuringVegetation/measuring_vegetation_2.php

[4]Elkhrachy, I., "Accuracy Assessment of Low-Cost Unmanned Aerial Vehicle (UAV) Photogrammetry," *Alexandria Engineering Journal,* Vol. 60, Pg. 5579-5590, 2021, URL: https://doi.org/10.1016/j.aej.2021.04.011

[5]Muhammad, M., Tahar, K. N., "Comprehensive Analysis of UAV Flight Parameters for High Resolution Topographic Mapping," *International Conference on Geomatics and Geospatial Technology,* Vol. 767, 2021, URL: https://iopscience.iop.org/article/10.1088/1755-1315/767/1/012001/pdf

[6]Awasthi, B., Regmi, P., Karki, S., Dhami, D. S., "Analyzing the Effect of Distribution Pattern and Number of GCPs on Overall Accuracy of UAV Photogrammetric Results," *Lecture Notes in Civil Engineering,* Vol. 51, Springer, 2020, URL: https://doi.org/10.1007/978-3-030-37393-1_29

[7]Akay, S. S., Ozcan, O., Sanli, F. B., Bayram, B., Gorum, T., "Assessing the Spatial Accuracy of UAV-Derived Products Based on Variation of Flight Altitudes," *Turkish Journal of Engineering*, Vol. 5, Pg. 35-40, 2021, URL: https://doi.org/10.31127/tuje.653631

[8]Pytharouli, S., Souter, J., Tziavou, O., "Unmanned Aerial Vehicle (UAV) Based Mapping in Engineering Surveys: Technical Considerations for Optimum Results," *Engineering Geology,* Vol. 232, Pg, 12-21, 2018, URL: https://doi.org/10.1016/j.enggeo.2017.11.004

[9]"Ground Control Points," *DJI Enterprise,* 2022, URL: https://enterprise-insights.dji.com/blog/ground-control-points

[10]Candido de Oliveira, H., Garcia, M. V. Y, "The Influence of Ground Control Points Configuration and Camera Calibration for DTM and Orthomosaic Generation Using Imagery Obtained from a Low-Cost UAV," *ISPRS Ann. Photogramm. Remote Sens. Spatial Inf. Sci.*, Vol., 1, Pg. 239–244, 2020, URL: https://doi.org/10.5194/isprs-annals-V-1-2020-239-2020

[11]Aguera-Vega, F., Carvajal-Ramirez, F., Martinez-Carricondo, P., "Assessment of Photogrammetric Mapping Accuracy Based on Variation Ground Control Points Number Using Unmanned Aerial Vehicle," *Measurement,* Vol. 98, Pg. 221-227, 2017, URL: https://doi.org/10.1016/j.measurement.2016.12.002

[12]Dimosthenis, C., Triantafyllou, A., Bib, S., Sarigannidis, P., "Data Acquisition and Analysis Methods in UAV-Based Applications for Precision Agriculture," *15th International Conference on Distributed Computing in Sensor Systems,* 2019, URL: https://doi.org/10.1109/DCOSS.2019.00080

[13] Candido de Oliveira, H., Garcia, M. V. Y, "The Influence of Flight Configuration, Camera Calibration, and Ground Control Points for Digital Terrain Model and Orthomosaic Generation Using Unmanned Aerial Vehicles Imagery," *Bulletin of Geodetic Sciences,* 2021, URL: https://doi.org/10.1590/s1982-21702021000200015

[14]"DJI Mavic 3M User Manual," URL: https://dl.djicdn.com/downloads/DJI_Mavic_3_Enterprise/20221216/DJI_Mavic_3M_User_Manual-EN.pdf

[15]Wierzbicki, D., Kedzierski, M., Fryskowska, A., "Assessment of the Influence of UAV Image Quality on the Orthophoto Production," *International Archives of the Photogrammetry, Remote Sensing, and Spatial Information Sciences,* Vol. XL-1/W4, 2015, URL: https://doi.org/10.5194/isprsarchives-XL-1-W4-1-2015

[16]"DJI Mavic 3M," *DJI Agriculture,* URL: https://ag.dji.com/mavic-3-m

[17]"DJI Mavic 3M Image Processing Guide," *DJI*, URL: https://dl.djicdn.com/downloads/DJI_Mavic_3_Enterprise/20230829/Mavic_3M_Image_Processing_Guide_EN.pdf

[18]"Agisoft Metashape User Manual," *Agisoft LLC,* Professional Edition, Version 1.5, 2019, URL: https://www.agisoft.com/pdf/metashape-pro_1_5_en.pdf